Molecular heat pump for rotational states

Article (Published Version)

Molecular heat pump for rotational states

C. Lazarou,[1,2] M. Keller,[1] and B. M. Garraway[1]
[1]*Department of Physics and Astronomy, University of Sussex, Falmer, Brighton, BN1 9QH, United Kingdom*
[2]*Department of Physics, Sofia University, James Bourchier 5 Boulevard, 1164 Sofia, Bulgaria*
(Received 15 July 2009; revised manuscript received 11 December 2009; published 27 January 2010)

In this work, we investigate the theory for three different unidirectional population-transfer schemes in trapped multilevel systems which can be utilized to cool molecular ions. The approach we use exploits the laser-induced coupling between the internal and motional degrees of freedom so that the internal state of a molecule can be mapped onto the motion of that molecule in an external trapping potential. By sympathetically cooling the translational motion back into its ground state, the mapping process can be employed as part of a cooling scheme for molecular rotational levels. This step is achieved through a common mode involving a laser-cooled atom trapped alongside the molecule. For the coherent mapping, we will focus on adiabatic passage techniques which may be expected to provide robust and efficient population transfers. By applying far-detuned chirped adiabatic rapid passage pulses, we are able to achieve an efficiency of better than 98% for realistic parameters and including spontaneous emission. Even though our main focus is on cooling molecular states, the analysis of the different adiabatic methods has general features which can be applied to atomic systems.

DOI: 10.1103/PhysRevA.81.013418 PACS number(s): 33.80.Be, 37.10.Mn

I. INTRODUCTION

The emerging field of cold molecules is a very vibrant topic in physics and physical chemistry. The considerable interest in this topic is related to the properties of cold molecules and their many potential applications. Cold molecules have been identified as attractive systems for ultrahigh-resolution spectroscopy [1,2] and quantum-information processing [3], for developing new time standards and testing fundamental physical theories such as the time variation of physical constants [4,5] and the existence of a dipole moment of the electron [6], and for measuring parity violation [7]. In chemistry, cold molecules are essential tools for exploring quantum-mechanical effects in chemical reactions. In contrast to atoms, molecules have a very complicated level structure that consists of vibrational and rotational states as well as electronic levels. This abundance of states is the main obstacle to the direct laser cooling of molecules. Usually, molecules do not provide the closed transitions required for cooling and nondestructive state-selective detection. This makes it impossible to perform direct spectroscopic measurements on *single* molecules—a standard technique in atomic physics. Additional complications result from the small energy differences between the rotational levels, leading to a thermal distribution of the population over the molecules' ro-vibrational states.

Despite important achievements [8–10], the control of molecular states has never caught up with that of atomic systems. However, there has been remarkable progress in the synthesis of ultracold alkali dimers from samples of ultracold atoms; see, e.g., Refs. [11–13]. Furthermore, methods which enable the preparation of more diverse (e.g., polyatomic) cold molecular species in their vibrational ground states have been successfully demonstrated. These methods include supersonic beam expansion followed by Stark deceleration [9], optical Stark deceleration [10], electrostatic velocity selection [14], collisional cooling in crossed molecular beams [15], and buffer gas cooling [8]. The vibrationally cold (but rotationally hot) states that result will be taken to be the starting point for the schemes described in this paper. The experimental advances which have enabled the production of these cold molecular states have inspired theoretical investigations of the cooling of molecules by laser pulses [16–20] or even by coupling molecules to an optical cavity [21]. Bartana *et al.* [18] used the electronic excited state as a heat reservoir in order to cool the vibrational states of the electronic ground state by means of short, shaped, laser pulses. In later work [19], they employed state selective optical pumping, hiding the target state in a dynamically trapped state. Through this, Bartana *et al.* achieved a vibrational ground-state population of 97% after only 25 vibration periods. A related scheme, investigated by Schirmer [16], increased the vibrational ground-state population to a similar level. These efforts to cool the internal degrees of freedom focus on the widely spaced vibrational states of molecules. In Ref. [20], Bartana *et al.* investigated the possibility of cooling the *rotational* degrees of freedom in a simplified model employing the same techniques. However, even though the results of their calculations are very promising, the model has limited application as it neglects the vibrational degree of freedom of the molecule.

In contrast to neutral molecules, ionized molecules can be sympathetically cooled by trapping them alongside atomic ions in a Paul trap. Under these conditions, state-sensitive ultracold chemical reactions have been measured [22,23] and high-resolution spectroscopy has been demonstrated on small ensembles [24]. Despite these achievements, the rotational degrees of freedom could not be controlled, but they led to new laser cooling schemes for the internal states of molecules [25,26] exploiting the unique properties of these systems.

In the present paper, we show that by means of purely coherent manipulations of internal states (i.e., rotational states) and by using sympathetic cooling of motional states, single molecular ions can be cooled close to their motional and rotational ground state. The internal vibration of the molecule needs to be initially cold in order for the final state to be cold in *all* its degrees of freedom. This initial state can be achieved using the existing methods described above. Then the cooling of the internal molecular state is achieved in three

steps: first a laser-cooled atomic ion is trapped alongside the molecule and a common mode of vibration is used to prepare the molecule in its motional ground state. Next, using adiabatic passage methods [27–36], the thermal internal state of the molecule can be mapped onto the molecule's motion in an external trapping field with high fidelity. During this mapping process, the internal (rotational) states are transferred to the ground state, whereas the molecule's motion is excited. Finally, the molecule's motion is sympathetically cooled back into its ground state using the common mode with a cooled atomic ion. By doing this without exciting other degrees of freedom, a molecule which is vibrationally, rotationally, and translationally cold can be obtained. The overall process is a kind of molecular "heat pump": the heat energy in the rotational degree of freedom is transferred by the coherent processes to the motional degree of freedom. This heat energy is in turn transferred to the environment by means of conventional cooling techniques, e.g., sideband cooling; this ensures that the process is unidirectional.

Vogelius *et al.* [25] investigated the cooling of molecular ions by coupling a single rotational state to the motion of the ion. By means of black-body radiation, the population is pumped into the rotational ground state resulting in a ground-state population of about 80% after a cooling time of the order of minutes. In this paper, we focus on the cooling process by employing techniques from coherent control providing much faster and more efficient cooling. The result is a robust and highly efficient cooling process which enables the deterministic manipulation of the internal states of molecules. We will examine adiabatic passage schemes which exhibit high fidelity in conjunction with relaxed requirements on the experimental parameters compared to direct Raman transitions. With cooling times of the order of milliseconds and final ground-state populations of more than 92%, the proposed scheme provides a fast and efficient method for preparing molecules in their ro-vibrational ground state.

Even though we focus here on the cooling of molecular rotational levels, the technique is also applicable to other multilevel systems. So the technique can also be employed in atoms with complicated level schemes or in more general ro-vibrational states of molecules.

The paper is organized as follows. In Sec. II, we present the model used for our calculations. To find the best adiabatic passage process for our application, we compare the results of numerical simulations for stimulated Raman adiabatic passage (STIRAP), Stark chirped Raman adiabatic passage (SCRAP), and chirped adiabatic rapid passage (CARP) in a Λ-type level system in Sec. III. We also choose parameter ranges which are relevant for a possible experimental implementation. Section IV contains the results for an extended level scheme, and in Sec. V we present our conclusions.

II. THE MODEL

The model we employ in this paper is based on the states of a quantum-mechanical rigid rotator which is a good approximation for the rotational states of small diatomic molecules. However, the techniques described here are applicable to most other level structures with the sole requirement that allowed Raman transitions between the states involved exist. In general,

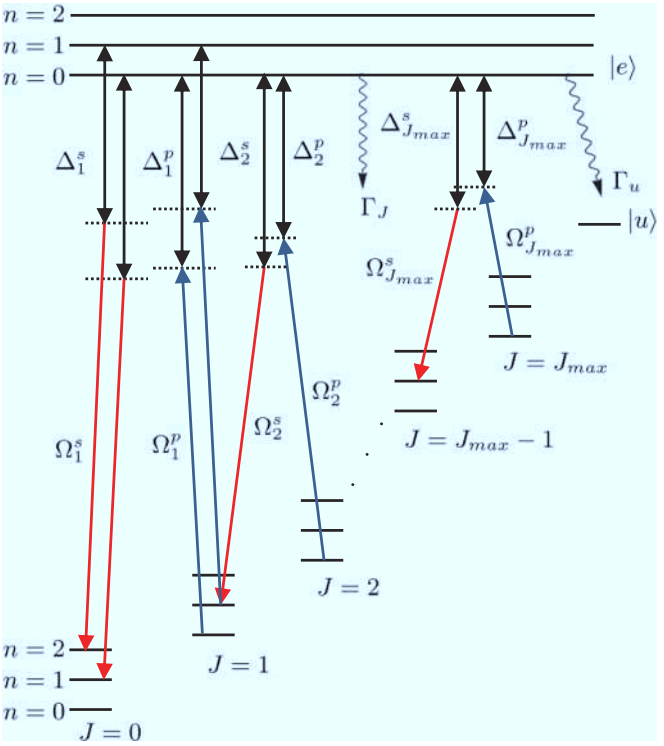

FIG. 1. (Color online) Overview of the molecular levels and the couplings which are included in the model. Near-resonant laser pulses are driving the transitions between the excited levels $|e,n\rangle$ and the rotational states $|J,n\rangle$. The excited state decays toward the states $|J\rangle$ at a rate Γ_J and toward the uncoupled state $|u\rangle$ at a rate Γ_u. The laser pulses have time-dependent Rabi frequencies $\Omega_J^{s,p}$ and are detuned from the relevant transition frequency by $\Delta_J^{s,p}$.

the method can be applied to ro-vibrational states of molecules as well as Zeeman and hyperfine levels. In order to simplify the discussion, and to avoid specializing to molecules with specific symmetries, we will not apply specific selection rules to the Raman transitions involved. Nevertheless, the results presented in this paper can be applied to a particular system by imposing the specific selection rules for that case with an appropriate relabeling of states. For example, we could utilize $\Delta J = 0, \pm 2$ for linear molecules.

We take the energy E_J of the rotational levels of the electronic ground state to be $E_J = BJ(J+1)$, with the rotational quantum number J and a rotational constant B. In order to limit the number of levels in our calculations, only rotational levels up to a cutoff are considered, i.e., $J \leqslant J_{\max}$. For typical, light, diatomic molecules at room temperature, only rotational states with $J < 20$ are significantly populated. This decreases to below ten states for rotational temperatures lower than about 50 K. This kind of temperature can be easily achieved by supersonic beam expansion [37]. In our scheme, the levels J are coupled by laser pulses to an electronically excited state $|e\rangle$ (see Fig. 1). From the excited state, the molecule can spontaneously decay back into the electronic ground state with a rate Γ_J. To represent the decay of the excited state into levels outside the system, e.g., rotational states with $J > J_{\max}$ or vibrationally excited states, an additional level $|u\rangle$ is also included in the model. The excited state can decay into this uncoupled state with a rate Γ_u.

The single molecule is trapped in a harmonic potential as provided by rf traps for molecular ions. The quantized motion of the molecule in the trapping potential gives rise to an equally spaced ladder of motional states in addition to the internal states of the molecule. To take the molecule's motion into account, we use the standard notation $|i,n\rangle$, with i representing the states $|J\rangle$, $|e\rangle$, and $|u\rangle$. The quantum number describing the motional state is n. As discussed in the Introduction, in order to prepare the molecule's motion in its ground state, it is trapped alongside one or more atomic ions which can be directly laser cooled. The two types of ion form a crystal-like structure due to their mutual Coulomb repulsion, which enables sympathetic cooling of the molecule. In experiments with two types of atomic ion, ground-state populations of better than 95% have been achieved [38]. In the molecular case, the minimal system would be one trapped molecular ion and one trapped atomic ion. In this case, we find that due to the frequency splitting of the motional modes, one mode (either the center of mass mode or the stretch mode) can be singled out and used for the proposed scheme. The other mode only imposes an additional limit on the laser-pulse length, as we will discuss later in this paper.

The laser-molecule interaction, in the rotating-wave approximation (RWA) [39], is described by the following Hamiltonian [40]:

$$\begin{aligned}\hat{H}(t) &= \hbar\nu\hat{a}^\dagger\hat{a} + \sum_{J=1}^{J_{\max}}\hbar\Delta_J^p(t)|e\rangle\langle e| \\ &+ \sum_{J=1}^{J_{\max}}\hbar\left[\Delta_J^p(t) - \Delta_J^s(t) + \nu\right]|J-1\rangle\langle J-1| \\ &+ \sum_{k=s,p}\left[\hat{H}_c^k(t) + \hat{H}_r^k(t) + \hat{H}_b^k(t)\right], \end{aligned} \tag{1}$$

where $\hat{H}_c^k(t)$ represents the carrier resonance [41] for either the pump ($k=p$), or the Stokes pulse ($k=s$), with

$$\begin{aligned}\hat{H}_c^p(t) &= \sum_{J=1}^{J_{\max}}\frac{\hbar\Omega_J^p(t)}{2}(\hat{\sigma}_+^J + \hat{\sigma}_-^J), \\ \hat{H}_c^s(t) &= \sum_{J=1}^{J_{\max}}\frac{\hbar\Omega_J^s(t)}{2}(\hat{\sigma}_+^{J-1} + \hat{\sigma}_-^{J-1}). \end{aligned} \tag{2}$$

The corresponding "red" sideband transitions in Eq. (1) are the $\hat{H}_r^k(t)$, which are given by

$$\begin{aligned}\hat{H}_r^p(t) &= \sum_{J=1}^{J_{\max}}\frac{\hbar\eta_J^p\Omega_J^p(t)}{2}(\hat{\sigma}_+^J\hat{a} + \hat{\sigma}_-^J\hat{a}^\dagger), \\ \hat{H}_r^s(t) &= \sum_{J=1}^{J_{\max}}\frac{\hbar\eta_J^s\Omega_J^s(t)}{2}(\hat{\sigma}_+^{J-1}\hat{a} + \hat{\sigma}_-^{J-1}\hat{a}^\dagger), \end{aligned} \tag{3}$$

and for the first "blue" sideband transitions, the $\hat{H}_b^k(t)$ are given by

$$\begin{aligned}\hat{H}_b^p(t) &= \sum_{J=1}^{J_{\max}}\frac{\hbar\eta_J^p\Omega_J^p(t)}{2}(\hat{\sigma}_+^J\hat{a}^\dagger + \hat{\sigma}_-^J\hat{a}), \\ \hat{H}_b^s(t) &= \sum_{J=1}^{J_{\max}}\frac{\hbar\eta_J^s\Omega_J^s(t)}{2}(\hat{\sigma}_+^{J-1}\hat{a}^\dagger + \hat{\sigma}_-^{J-1}\hat{a}). \end{aligned} \tag{4}$$

In Eqs. (1)–(4), the secular frequency of the molecule in the external trapping potential is ν, and η_J^k are the corresponding Lamb-Dicke parameters [41]. The detuning between the kth laser frequency ω_J^k and the transition frequency ω_{eJ} of the $|J\rangle \rightarrow |e\rangle$ transition is $\Delta_J^p(t) = \omega_{eJ} - \omega_J^p(t)$ and $\Delta_J^s(t) = \omega_{eJ-1} - \omega_J^s(t) - \nu$. The raising operator for the internal states is $\hat{\sigma}_+^J = |e\rangle\langle J|$, and the lowering operator is $\hat{\sigma}_-^J = |J\rangle\langle e|$. The creation and annihilation operators for the motional number states $|n\rangle$ are $\hat{a}^\dagger$ and $\hat{a}$, respectively. Note that we work in an interaction representation with explicit time dependence removed, and we keep both the resonant and nonresonant couplings. The reason for this is that in pursuing the adiabatic limit in Sec. III, we will consider "strong" Rabi frequencies ($\Omega_J^k \sim \nu$) which do not allow us to make a second RWA on the Hamiltonians for the sideband transitions.

We start our calculations with a molecule in an internal thermal state such that it is already cooled in its internal vibrational mode (e.g., by the methods mentioned in the Introduction) and such that the excited state $|e\rangle$ is not populated. We also assume that the molecule's vibrational motion in the trap has been cooled (e.g., by sympathetic sideband cooling [38]) so that only the manifold of rotational states $|J,0\rangle$ are populated. The density matrix of this initial state is given by

$$\rho_{\text{init}} = \frac{1}{Z}\sum_{J=0}^{J_{\max}}(2J+1)e^{-\beta BJ(J+1)}|J,0\rangle\langle 0,J|, \tag{5}$$

where $J_{\max}$ is the cutoff introduced for the numerical calculations. The normalization factor Z is given by $Z = \sum_{J=0}^{J_{\max}}(2J+1)\,e^{-\beta BJ(J+1)}$ with $\beta = 1/(k_B T)$, and with T as the internal rotational temperature of the molecule.

Starting from such an initial distribution, we will apply coherent control techniques to transfer population between the different states. We aim to have a state mapping of the form

$$\sum_{J=0}^{J_{\max}}P_{J,0}|J,0\rangle\langle 0,J| \rightarrow \sum_{n=0}^{J_{\max}}P_{0,n}|0,n\rangle\langle n,0|, \tag{6}$$

where $P_{J,0} = P_{0,n} = e^{-\beta BJ(J+1)}/Z$ are the populations of the initial states $|J,n=0\rangle$ and the final target states $|J=0,n\rangle$, respectively. A sequence of pulses will be used to map population in each J state to a corresponding n state with $J=0$.

Throughout this work, we assume that the system is initially prepared in a state given by Eq. (5) and derive the requirements for achieving the state mapping in Eq. (6), i.e., after completion of a number of the coherent pulse sequences. Thus we obtain a superposition of just the motional states which can then be cooled to the motional ground state $|J=0,n=0\rangle$ by applying the sympathetic cooling [38]. [The state mapping (6) can also be employed for nondestructive state detection, e.g., by measuring the initial thermal distribution (5). By coupling the electronic state of an atom trapped alongside the molecules to its motion, the mapped state can be read out.] For the coherent mapping, the key idea is to use pairs of pulses, $\Omega_J^p(t)$ and $\Omega_J^s(t)$, to induce population transfer between the states $|J,n\rangle$ and $|J-1,n+1\rangle$, see Fig. 1. For this step, it is important to have a resonance, so that additional states do

not get strongly involved and disturb the mapping. Here, the resonance is arranged so that the quantity $J+n$ is conserved at each step. (Although this is the simplest way to make the mapping, it would not be the only way, as we only require the transfer of population between unique pairs of states.)

Repeating the $J,n \longrightarrow J-1,n+1$ step $J_{\max}$ times, where in each step, J is decreased by one, the distribution of population can be moved to the $J=0$ motional states as in Eq. (6). Since states with $n \neq 0$ are involved in the intermediate steps, it is clear that if we do not start in the motional ground state, the final state need not be entirely $J=0$. However, when we start in the motional ground state (i.e., $n=0$), the population transfer is unidirectional. Hence, the population is transferred solely to the lower lying rotational states.

In our analysis, we numerically integrate the master equation for the density matrix $\rho(t)$:

$$\frac{d\rho(t)}{dt} = -\mathrm{i}[\hat{H}(t),\rho(t)] + \hat{\mathcal{L}}(\rho(t)) + \hat{\mathcal{L}}_u(\rho(t)). \tag{7}$$

The Hamiltonian $\hat{H}(t)$ is given in Eq. (1). The two Liouville terms $\hat{\mathcal{L}}(\rho(t))$ and $\hat{\mathcal{L}}_u(\rho(t))$ describe the irreversible decay of the excited electronic state $|e\rangle$ to the rotational levels $|J\rangle$ of the electronic and vibrational ground state,

$$\hat{\mathcal{L}}(\rho(t)) = -\sum_{J=0}^{J_{\max}} \frac{\Gamma_J}{2}[\rho(t)\hat{\sigma}_+^J\hat{\sigma}_-^J + \hat{\sigma}_+^J\hat{\sigma}_-^J\rho(t) - 2\hat{\sigma}_-^J\rho(t)\hat{\sigma}_+^J], \tag{8}$$

and the decay out of the system, i.e., to the uncoupled state $|u\rangle$,

$$\hat{\mathcal{L}}_u(\rho(t)) = -\frac{\Gamma_u}{2}[\rho(t)\hat{\sigma}_+^u\hat{\sigma}_-^u + \hat{\sigma}_+^u\hat{\sigma}_-^u\rho(t) - 2\hat{\sigma}_-^u\rho(t)\hat{\sigma}_+^u]. \tag{9}$$

In Eq. (9) the raising and lowering operators $\hat{\sigma}_\pm^u$ have the same form as $\hat{\sigma}_\pm^J$, with the substitution $|J\rangle \rightarrow |u\rangle$.

We will assume that the laser pulses are Gaussian, with a fixed width T and Rabi frequencies

$$\begin{aligned}\Omega_J^p(t) &= \Omega_0^p e^{-[t-3\tau-(J_{\max}-J)\tilde{\tau}]^2/T^2},\\ \Omega_J^s(t) &= \Omega_0^s e^{-[t-\tau-(J_{\max}-J)\tilde{\tau}]^2/T^2},\end{aligned} \tag{10}$$

where $J=1,\ldots,J_{\max}$. The delay between the two pulses $\Omega_J^s(t)$ and $\Omega_J^p(t)$ that drive the transition $|J\rangle \rightarrow |J-1\rangle$ is 2τ, whereas the delay between the J and $J+1$ pulse pair is $\tilde{\tau}$. The corresponding detunings will be either constants or have the form of time-dependent frequency chirps. We take all the Lamb-Dicke parameters to be the same, i.e., $\eta_J^k = \eta$, and for simplicity we assume that the decay rates are the same, i.e., $\Gamma_J = \Gamma_u = \Gamma$. In order to compare the three methods (STIRAP, SCRAP, and CARP) in Sec. III, we characterize the population-transfer efficiency by a parameter ϵ representing the total population of the rotational ground state after the transfer:

$$\epsilon = \sum_{n=0}^{J_{\max}} P_{0,n}(t=\infty), \tag{11}$$

where $P_{0,n}(t=\infty)$ is the population of the $|J=0,n\rangle$ state after the transfer. For an efficient state mapping, the ground-state population ($J=0$) will have increased. However, if the initial state also has some population in the $|J=0,n=0\rangle$ state, the efficiency ϵ may also decrease due to laser-induced transfer out of $|J=0,n=0\rangle$. Thus the definition (11) is a measure not only for the transfer efficiency but also for the unidirectionality of the mapping process. For ideal state mapping, the efficiency measure reaches the limit $\epsilon=1$. In order to test the various passage methods in the next section, the initial state is taken to be a mixture of 70% rotationally excited states ($J>0$) and 30% ground state ($J=0$) population for each adiabatic method. This approach will test how unidirectional the scheme is.

III. ADIABATIC PASSAGE METHODS

To transfer the population from the state $|J,n\rangle$ to $|J-1,n+1\rangle$, various coherent processes can be employed. Here we focus on stimulated Raman adiabatic passage (STIRAP) [34,42,43], Stark chirped Raman adiabatic passage (SCRAP or SIARP) [31–33], and chirped adiabatic rapid passage (CARP) [27–30], which offer highly efficient population transfer in combination with robustness against variations of the pulse parameters. In order to simplify the numerical simulations, we first investigate these processes in a system with just two rotational levels. That is, we examine in detail a single step in our multipulse coherent transfer scheme. In this case, the most important states are the two lowest motional states for $J=0$ and the lowest ($n=0$) motional state for $J=1$ (see Fig. 2). However, to include the off-resonant effects, all nine of the states shown in Fig. 2 are included in the numerical

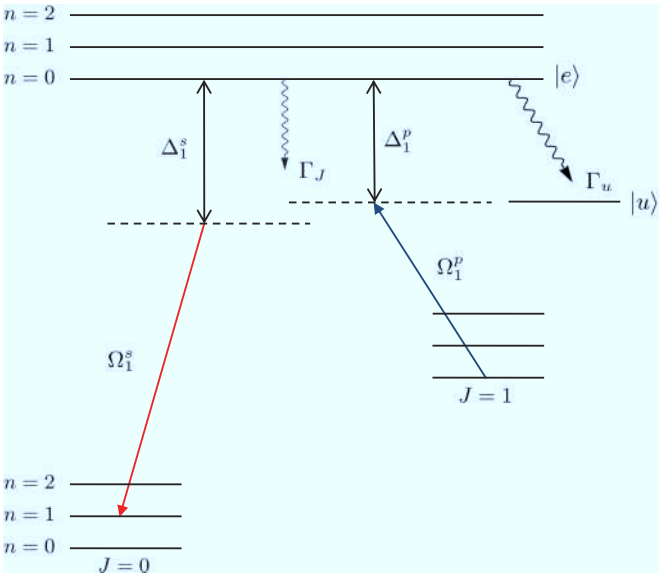

FIG. 2. (Color online) Basic Λ configuration used to investigate the transfer efficiency of various adiabatic passage schemes in Sec. III. The pump and Stokes pulses, $\Omega_1^p(t)$ and $\Omega_0^s(t)$, respectively, will induce a two-photon Raman transition (which may be chirped) from state $|n=0,J=1\rangle$ to state $|n=1,J=0\rangle$. The best results are obtained if the initial population in $|n=0,J=0\rangle$ remains there. The off-resonant intermediate states $|e,0\rangle$ decays toward the two rotational states and toward the uncoupled state $|u\rangle$ at a rate Γ_u. The decay rate Γ_J represents decay from the levels e to the levels n,J. Other off-resonant states are included as shown.

calculation. We choose parameter ranges which are relevant for an experimental implementation. The electronically excited state can decay to both rotational states as well as into the uncoupled state $|u\rangle$.

A. Stimulated Raman adiabatic passage

STIRAP is widely used in the optical control of molecules [34,35,44] where a Stokes pulse and a pump pulse are used in a "counterintuitive" order to transfer the population between two states. The main requirement for STIRAP is the two-photon resonance condition which corresponds to $\Delta_1^p(t) = \Delta_1^s(t)$ for a transition on a motional sideband (see Fig. 1). In addition to this, the pulse area must be large, $\Omega_0 T \gg 1$, and the delay between the Stokes and pump pulse must be of the order of the pulse width, $\tau \approx T$, to ensure the adiabatic evolution of the system. Another constraint arises from the necessity to address particular motional sidebands. The narrow splitting of the motional states imposes the use of laser pulses with narrow bandwidth $\nu T \gg 1$ [36]. Fast pulses will inevitably result in the coupling of the target state to other, close-lying states. This in turn will reduce the transfer efficiency. Furthermore, the resolved sideband condition [41] requires that the Rabi frequencies are small compared to the trap frequency, i.e., $\Omega_0 \ll \nu$. Thus, only slow and weak pulses can be used which, as we will see, substantially reduces the efficiency of STIRAP. However, this can be overcome by employing other adiabatic passage schemes as described below.

In Fig. 3(a), the transfer efficiency ϵ is plotted for different pulse widths T and delay times τ. As mentioned above, the initial mixed state is described by the populations $P_{0,0}(-\infty) = 0.3$ and $P_{1,0}(-\infty) = 0.7$. The chosen decay rate of $\Gamma = 0.01\nu$ is in the typical range of values for the decay rate of an electronically excited molecule, when compared to a typical trap frequency ν (of the order of several MHz). The results in Fig. 3(a) show that the efficiency ϵ is below 76%. The performance of STIRAP for short pulses is relatively poor due to the violation of the adiabaticity requirement ($\Omega_0 T \gg 1$) and the limitation on the Rabi frequency Ω_0 posed by the resolved sideband condition ($\Omega_0 \ll \nu$). For long pulses, the efficiency of STIRAP is compromised by the spontaneous decay $\Gamma_{u,J}$, so the compensation of small Rabi frequencies by long laser pulses is not an option. Therefore, the efficiency of STIRAP in this parameter range is low, and the population transfer is governed by optical pumping rather than coherent evolution. This is particularly visible in the plateau region for $\tau \gg T$. In this regime, the pulse delay is too large to sustain the adiabatic evolution of the system, which results in a net loss of the ground-state population. Highly efficient, fast STIRAP between motional states requires large motional frequencies which are beyond current ion-trap technology.

We can try to suppress the excited-state population by detuning the Raman transition from the excited state. However, it has been known for some time that detuning adversely affects the STIRAP process in the absence of decay [45]. With decay present, one has to consider the balance of the adverse effect of detuning against a possible reduction in spontaneous emission from the excited state of a model Λ system. Studies with such systems support the suggestion that the minimal

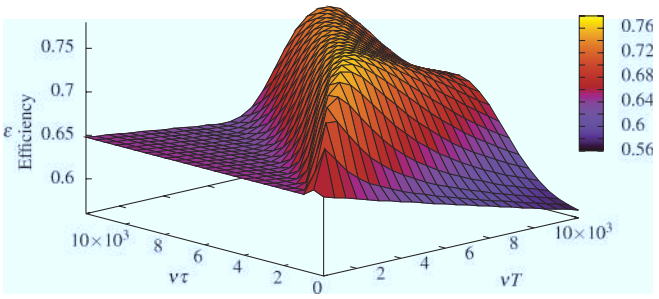

(a)

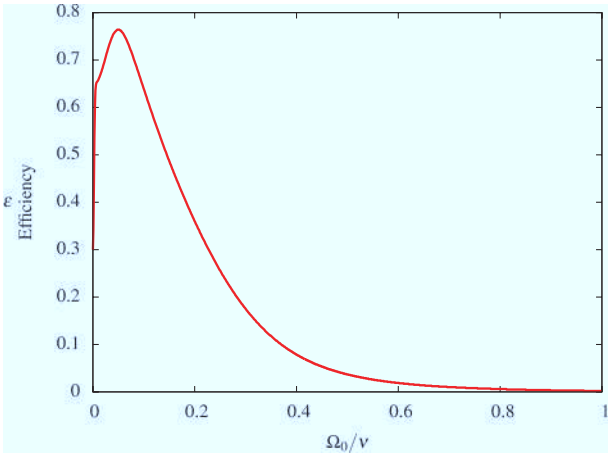

(b)

FIG. 3. (Color online) (a) Population transfer for STIRAP with different delay times τ and pulse widths T. The calculations are for the Λ system in Fig. 2. The Rabi frequency is $\Omega_0 = \nu/20$. (b) Efficiency as a function of Rabi frequency for $T = 4500/\nu$ and $\tau = 3500/\nu$. In (a) and (b), the pump and Stokes pulse detunings are $\Delta_1^p = \Delta_1^s = 0$ and the other parameters are $\Gamma_J = \Gamma_u = 0.01\nu$, $\eta = 0.1$, $P_{0,0}(-\infty) = 0.3$, and $P_{1,0}(-\infty) = 0.7$.

losses (for moderate decay rates) are found by remaining on resonance [34,46,47]. Figure 4 shows how the efficiency of STIRAP drops, for our model system, as we detune from resonance. The parameters are those for Fig. 3(b), with the Rabi frequency Ω_0 chosen to be at the peak of efficiency in Fig. 3(b). We see that both with and without decay processes, it is best to be resonant. In the case $\Gamma_J = 0$, the resonance is much sharper, however.

To exploit the adiabatic evolution of the system and to suppress the excited-state population by far detuning the Raman transition leads us to Stark chirped Raman adiabatic passage (SCRAP) and chirped adiabatic rapid passage (CARP), which will be discussed in Secs. III B and III C. In the limit of far detuning, the excited state population is strongly suppressed and the system's dynamics are effectively that of a two-level system [48]. The effective Raman coupling between the states $|J, n\rangle$ and $|J-1, n+1\rangle$ is

$$\Omega_J(t) = \frac{\eta \Omega_J^p(t) \Omega_J^s(t)}{\Delta_J^p(t)}, \tag{12}$$

and the effective splitting of the coupled rotational levels is

$$\Delta_J(t) = \delta_J(t) + S_J^s(t) - S_J^p(t), \tag{13}$$

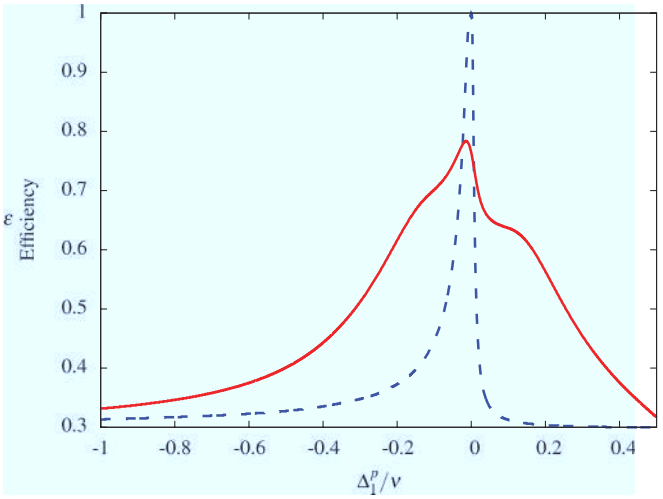

FIG. 4. (Color online) Efficiency of the STIRAP process as a function of detuning Δ_1^p $(= \Delta_1^s)$, with decay, $\Gamma_J = \Gamma_u = 0.01\nu$ (solid line), and without decay, $\Gamma_J = \Gamma_u = 0$ (dashed line). The other parameters are as in Fig. 3 with the best values taken for $T = 4500/\nu$, $\tau = 3500/\nu$, and $\Omega_0 = \nu/20$.

with the effective two-photon Raman detuning $\delta_J(t) = \Delta_J^s(t) - \Delta_J^p(t)$, and the two Stark shifts $S_J^s(t) = [\eta\Omega_J^s(t)]^2/4\Delta_J^s(t)$ and $S_J^p(t) = [\Omega_J^p(t)]^2/4\Delta_J^p(t)$ induced by the Stokes and pump pulse, respectively.

Within this effective two-level model, adiabatic rapid passage techniques (ARP) [30] can be applied. The main idea behind ARP is to drive the system through the resonance $(\Delta_J = 0)$ adiabatically, to achieve a complete population transfer. The technique of Stark chirped Raman adiabatic passage (SCRAP) [31–33] takes advantage of the Stark shifts, whereas the chirped adiabatic rapid passage (CARP) [27–30] uses overlapping laser pulses along with frequency chirps to transfer the population. We turn to these methods in the next sections.

B. Stark chirped Raman adiabatic passage

For the case of SCRAP (earlier known as self-induced-adiabatic passage, or SIARP [31]), the laser pulses are engineered so that the system undergoes an avoided level crossing $(\Delta_J = 0)$ near a maximum of the effective coupling $\Omega_J(t)$ induced by the Stark shifts due to the delay of the pump and Stokes pulses. In order to obtain an efficient population transfer, the system needs to evolve adiabatically in the crossing region [33]. For Gaussian pulses, this leads to the condition

$$\Omega_0^2 T^2 \gg |\tau|\left|\Delta_J^p\right| \exp(2\tau^2/T^2). \tag{14}$$

Figure 5(a) shows the efficiency ϵ for various Rabi frequencies and pulse delays for a decay rate of $\Gamma = 0.01\nu$ and a fixed pulse length of $T = 800/\nu$. The behavior described by the adiabaticity requirement is clearly visible. For a fixed Rabi frequency, the efficiency decreases with increasing pulse delay τ as predicted by Eq. (14). The improvement due to increased Rabi frequency is also evident. However, for large Rabi frequencies, the pulse violates the resolved sideband condition $\Omega_J(t) \ll \nu$, leading to a sudden deterioration of the

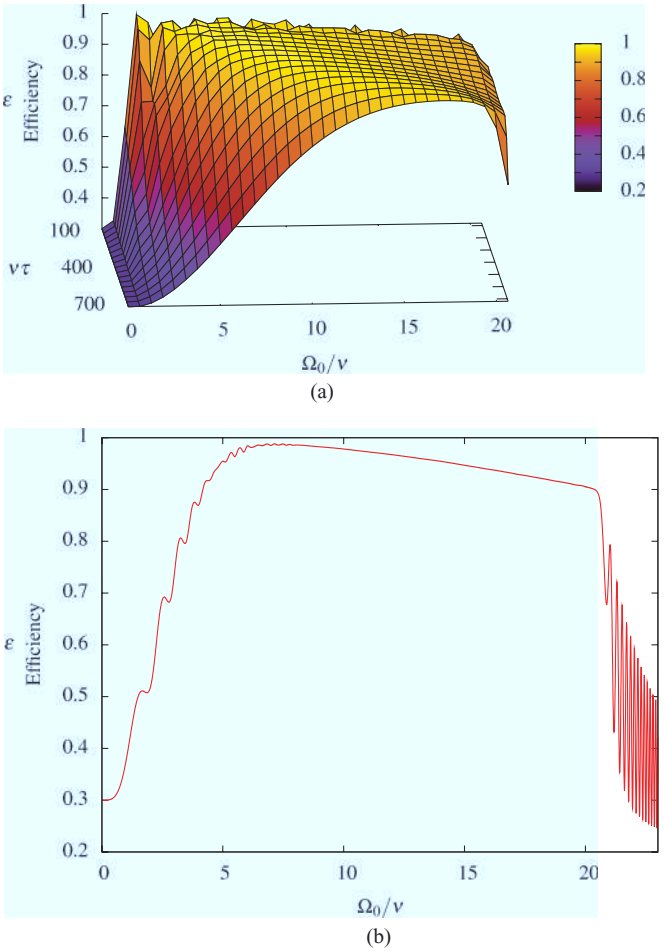

FIG. 5. (Color online) (a) Efficiency for SCRAP for different Rabi frequencies Ω_0 and delay times τ for the Λ system in Fig. 2. The pulse width is $T = 800/\nu$ and the pump and Stokes pulse detunings are $\Delta_1^p = \Delta_1^s = 100\nu$. (b) Efficiency for a delay $\tau = 320/\nu$. Other parameters are as in Fig. 3(a).

efficiency ϵ at large intensities, see Fig. 5(b). For small Rabi frequencies, the efficiency ϵ strongly depends on the delay times. For $\tau < 80/\nu$, the method is not robust. As the effective decay rate increases with increasing Rabi frequencies, the efficiency slowly degrades for greater laser intensity. This leads to a ridge in the τ-Ω diagram. Because the efficiency depends on the pulse delay and the Rabi frequency, accurate knowledge of these pulse parameters is required. This can be moderated by increasing the detuning of the laser pulses. Because the constraints on the pulse length are less severe than for STIRAP, the population transfer can be faster with SCRAP. Together with the far detuning, this leads to an improved robustness against the detrimental effect of spontaneous decay [49].

C. Chirped adiabatic rapid passage

Another way of achieving an adiabatic population transfer is the application of simultaneous pump and Stokes pulses $(\tau = 0)$ with one laser having a frequency chirp. This is a Raman chirped adiabatic passage, sometimes called RCAP [28], though here we refer to it as chirped adiabatic rapid passage (in a Λ system) or CARP. With this system, the Stark

shifts are eliminated, and the detuning $\Delta_J(t)$ reads

$$\Delta_J(t) = \delta_J(t) = \alpha[t - (J_{\max} - J)\tilde{\tau}]. \quad (15)$$

In order to ensure the adiabatic evolution, the chirp rate α needs to fulfill $|\alpha| \ll \Omega_J^2$ and $|\alpha|\, T^2 \gg 1$ [with the two-photon Rabi frequency Ω_J given by Eq. (12)]. These conditions arise from a Landau-Zener adiabaticity and from requiring completion of a Landau-Zener transfer within the time scale of the pulse. Because there is no limit on the pulse duration arising directly from the adiabaticity requirements, the transition can be fast: it is only limited by the narrow bandwidth condition $\nu T \gg 1$ [30]. This in turn reduces the susceptibility to spontaneous emission. The resolved sideband condition [41] requires that $\nu \gg \Omega_J(t)$, which is easy to satisfy since the system is in the far-detuned limit $\Delta_J^p \gg \Omega_0$. Under these conditions, the population transferred to the target state can be estimated with the Landau-Zener formula [50,51]

$$P_{J-1;n+1}(\infty) = P_{J,n}(-\infty)(1 - e^{-\pi\Lambda_J}), \quad (16)$$

where $\Lambda_J = \Omega_J(0)^2/2|\alpha| = \eta^2\Omega_0^4/[2(\Delta_J^p)^2|\alpha|]$. This behavior is confirmed by our numerical simulation [see Fig. 6(a)]. It shows the simulated efficiency for different Rabi frequencies and chirp rates for a system initially in a state with $P_{0,0}(-\infty) = 0.3$ and $P_{1,0}(-\infty) = 0.7$.

The efficiency increases rapidly with increasing Rabi frequency Ω_0 until it reaches a plateau. In this region, the transfer efficiency is well above 98%. For small Rabi frequencies, the efficiency ϵ deteriorates with increasing chirp rate. However, this effect diminishes for large pump intensities. Similar to SCRAP, the increase in the effective decay rate for high Rabi frequencies leads to a slow degradation of the transfer efficiency for large pulse intensities. For very high laser intensities, the efficiency rapidly drops due to the violation of the resolved sideband condition $\Omega_J(0) \ll \nu$. In a different parameter regime, that of small chirp rates $\alpha \ll 10^{-5}\nu^2$, the efficiency oscillates with changing Rabi frequency, see Fig. 6(b). Here the evolution is governed by Rabi oscillations between the two rotational states, which together with the finite pulse length leads to large fluctuations in the efficiency. In this regime, a very precise control of the laser pulses is required, so CARP is not robust for very small chirp rates. For large Rabi frequencies, the efficiency is essentially independent of the chirp rate, and CARP provides the best robustness against uncertainties in the pulse parameters.

D. Comparison of the adiabatic passage methods

Both of the adiabatic rapid passage methods, SCRAP and CARP, provide fast population transfer. Together with the large detuning of the Raman transition from the excited state, they provide robustness against the adverse effect of spontaneous emission. This is clearly evident in Fig. 7, where the efficiency of the three methods is plotted against the decay rate. In this figure, the values of the parameters Ω_0, T, and τ are optimized for $\Gamma = 0.01\nu$ and the detunings given. (In the case of CARP, the value of α is also optimal.) The same optimal values have been used for fixed parameters in Figs. 3–6. The parameter Γ has been fixed to a reasonable value for diatomic molecules like N_2^+ or CO^+. This optimization gives a fairly wide range of parameters in Fig. 7.

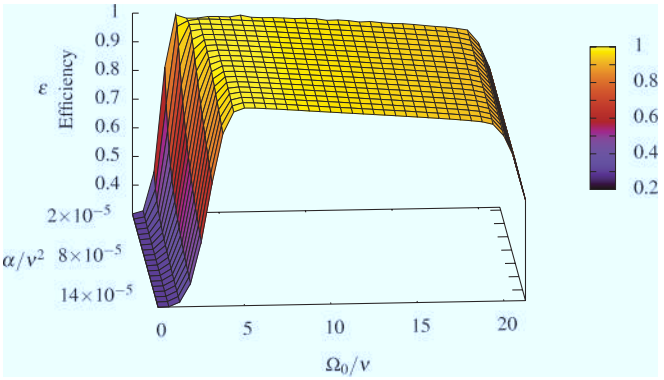

(a)

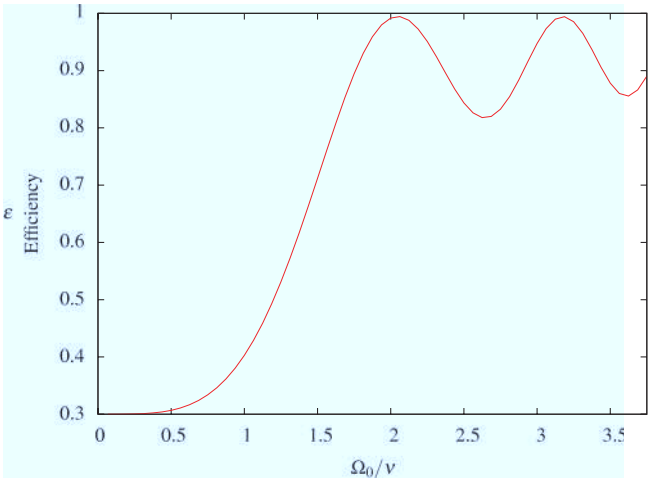

(b)

FIG. 6. (Color online) (a) Efficiency of CARP for different Rabi frequencies Ω_0 and chirp rates α for the Λ system in Fig. 2. The delay is $\tau = 0$, the pulse width is $T = 800/\nu$, and the Stokes pulse detuning is given by $\Delta_1^s = \Delta_1^p - \alpha t$. (b) Efficiency as a function of Rabi frequency Ω_0 for a small chirp rate $\alpha = 8 \times 10^{-6}\nu^2$. Other parameters are as in Fig. 3(a) with pump pulse detuning $\Delta_1^p = 100\nu$.

Figure 7 also shows that even though STIRAP is efficient for small decay rates, it decreases rapidly for larger decay rates. SCRAP and CARP are far more efficient, and their suppression of the excited-state population exceeds that of STIRAP within the limits imposed by the experimental requirements. Even though SCRAP and CARP exhibit similar efficiencies, CARP is more robust against uncertainties in the laser-pulse parameters. Hence, we use CARP for our investigation of the population transfer in a multilevel system with $J_{\max} = 5$ in the next section.

IV. CHIRPED ADIABATIC RAPID PASSAGE IN A MULTILEVEL SYSTEM ($J_{\max} > 1$)

Having derived the conditions for efficient population transfer with chirped two-photon Raman transitions, we turn now to systems where we include a larger number of rotational states in the calculation ($J_{\max} > 1$). Consequently the mapping

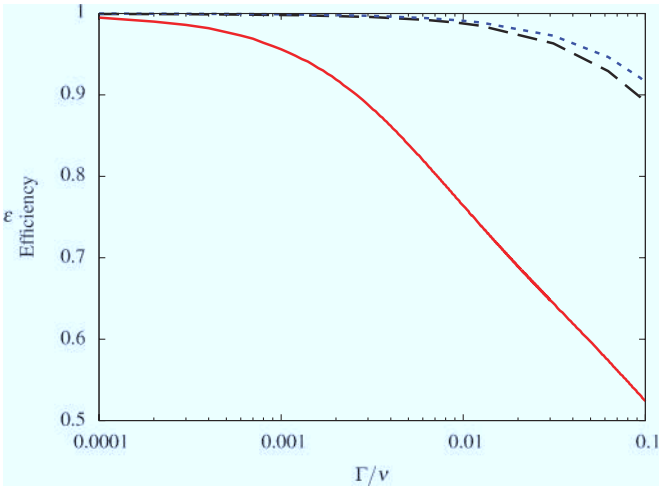

FIG. 7. (Color online) Population transfer for the Λ configuration of Fig. 2, for different decay rates $\Gamma = \Gamma_J = \Gamma_u$ and the three methods we consider. The parameters are optimized at $\Gamma_J = \Gamma_u = 0.01\nu$ for each of the three methods and are listed separately in the following. For STIRAP (solid line): $\Omega_0 = \nu/20$, $T = 4500/\nu$, $\tau = 3500/\nu$, and $\Delta_1^p = \Delta_1^s = 0$. For SCRAP (dashed line): $\Omega_0 = 7.5\nu$, $T = 800/\nu$, $\tau = 320/\nu$, and $\Delta_1^p = \Delta_1^s = 100\nu$. For CARP (dotted line): $\Omega_0 = 5\nu$, $T = 800/\nu$, $\tau = 0$, $\Delta_1^p = 100\nu$, and $\Delta_1^s = \Delta_1^p - \alpha t$ with $\alpha = 4.69 \times 10^{-5}\nu^2$. Other parameters which are fixed for all three cases are $J_{\max} = 1$, $n_{\max} = 2$, $\eta = 0.1$, $P_{0,0}(-\infty) = 0.3$, and $P_{1,0}(-\infty) = 0.7$.

process involves multiple ($J_{\max}$) pairs of laser pulses. We investigate the state mapping given in Eq. (6) for a thermal initial state distribution with $\beta B = 0.15$. This corresponds to a system where approximately six rotational levels are significantly populated, and consequently we will take $J_{\max} = 5$. In our simulation, we use a Lamb-Dicke parameter of $\eta = 0.1$ and a decay rate of $\Gamma = 0.01\nu$, which for realistic trap frequencies (of the order of a few MHz) corresponds to typical decay rates of electronically excited states of diatomic molecules. The pump laser is detuned by $\Delta_J^p = 100\nu$, and the Stokes laser is chirped with the rate $\alpha = 16 \times 10^{-5}\nu^2$. Both lasers have a peak Rabi frequency of $\Omega_0 = 5\nu$, a pulse length of $T = 800/\nu$, and a delay between successive pulse pairs of $\tilde{\tau} = 4800/\nu$. These parameters were chosen on the basis of the simulations with two rotational levels (Sec. III) and realistic experimental parameters.

In Fig. 8(a), the initial population distribution over all states $|J, n\rangle$ is plotted, along with the final distribution in Fig. 8(b). Apart from some small population loss, see Fig. 9, and some weak scattering of population into states other than the states $|0, n\rangle$, the two distributions agree very well. The total population transferred into the rotational ground state is 92%, while the total population loss into the uncoupled states is only 1.5%.

The remaining 6.5% of the total population is mostly left in the initial states $|J > 0, 0\rangle$ [see Fig. 8(b)]. Losses due to spontaneous emission can be further reduced by increasing the detuning. The population which remained in the higher, coupled rotational states $|J > 0, 0\rangle$ can be transferred into the ground state by sympathetically cooling the molecule's motion and reapplying the cooling pulse sequence. Using this approach, the population of the ground state can be even further

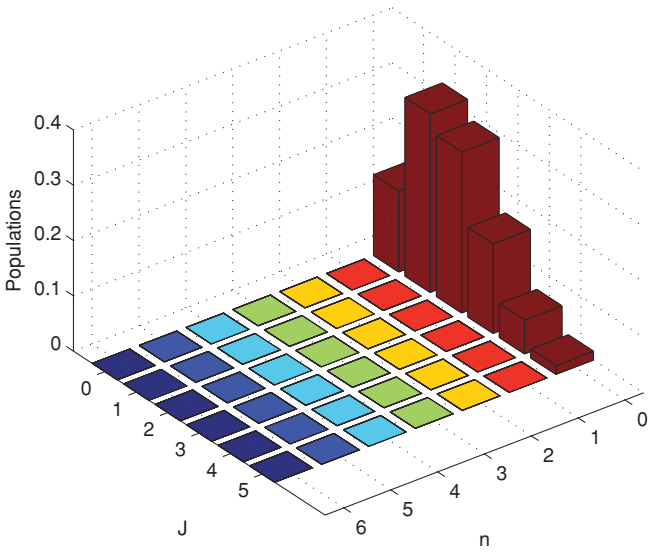

(a) Initial population distribution.

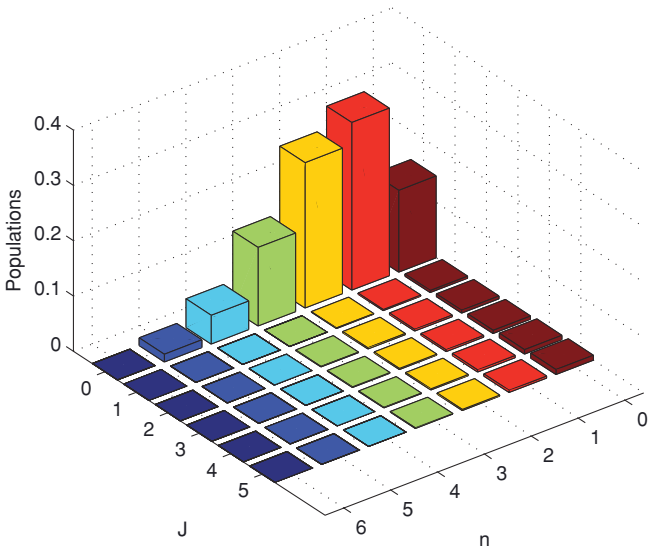

(b) Final population distribution.

FIG. 8. (Color online) (a) Initial thermal distribution for a system with $J_{\max} = 5$ and $\beta B = 0.15$, and (b) the final population distribution after the completion of five sequential chirped two-photon Raman transitions. The detuning for the pump pulse is $\Delta_J^p = 100\nu$, the Rabi frequency is $\Omega_0 T = 5\nu$, and all the decay rates are equal to $\Gamma_J = \Gamma_u = 0.01\nu$. Other parameters are $\eta = 0.1$, $\tau = 0$, $\tilde{\tau} = 4800/\nu$, $\alpha = 16 \times 10^{-5}\nu^2$, $T = 800/\nu$, and $n_{\max} = 6$.

increased from 92% to above 98.4% with a total loss into the uncoupled state of only 1.6%. Additional simulations with $\Delta_J^p = 200\nu$ and $10^3\nu$, resulted in higher efficiencies, 95.7% and 98.9%, respectively. The corresponding losses are less than 0.9% for $\Delta_J^p = 200\nu$ and 0.2% for $\Delta_J^p = 10^3\nu$.

For large numbers of populated states, the transfer efficiency can be estimated with the following equation:

$$P_{\text{total}} \approx \sum_{J=0}^{J_{\max}} P(J_{\max} - J)\epsilon^{J_{\max}-J}, \tag{17}$$

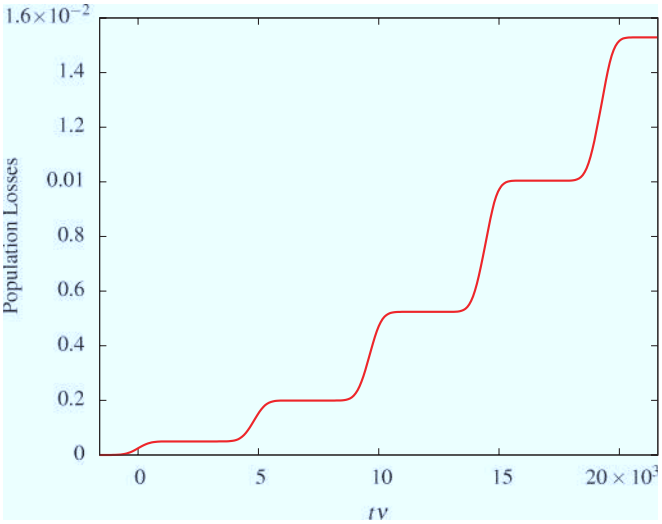

FIG. 9. (Color online) The (small) population loss as a function of time for the two-photon chirped Raman passage in a system with $J_{\max} = 5$, see Fig. 8. The detuning for the pump pulse is equal to $\Delta_1^p = 100\nu$ and the Rabi frequency is $\Omega_0 = 5\nu$. Other parameters are as in Fig. 8.

where ϵ is the transfer efficiency for the simple Λ system, and $P(J)$ is the initial population distribution (5). This agrees well with our numerical simulation of six rotational levels.

Starting from a vibrationally cold system, these values of the efficiency ϵ show that we can reach the motional and rotational ground state of molecules [52]. For a CO^+ ion with a rotational temperature of $T \approx 100$ K, the first 15 rotational levels are significantly occupied initially with a ground-state population of only 3%. By applying the CARP state mapping with a detuning of $\Delta_J^p = 100\nu$ and taking the selection rule $\Delta J = 0, \pm 2$ into account, the population of the two lowest lying states can be increased to 85%. Using a detuning of $\Delta_J^p = 10^3\nu$, this can be improved to 97.8% for a single cooling cycle. For a trap frequency of 4 MHz, this cooling cycle will be completed within 10 ms.

V. CONCLUSION

In this work, we presented an efficient method for cooling the internal states of molecules by means of coherent processes (and sympathetic cooling) thus suppressing the problematic spontaneous decay into uncoupled states. By coupling the internal molecular state to the motion of the molecule, that internal state can be mapped onto a motional state. Utilizing this, the *internal* state is cooled close to its ground state if the molecule's motion was initially reduced to the motional ground state through sympathetic cooling. Ultimately all the degrees of freedom of the molecule can be cooled by the application of sympathetic cooling to the final motional excitation. Due to its high efficiency, the method presented here is not only useful in cooling the internal state, but also can be employed to detect the internal state of the molecule by measuring its motional state with an atom which is trapped alongside.

We have studied various adiabatic methods for a range of laser-pulse parameters which are relevant for an experimental implementation of this cooling scheme. The motion of the ion imposes restrictions on the dynamics of the population-transfer process which severely limit the possible parameter range for the laser pulses. For the near-resonant method (STIRAP), population-transfer efficiency is very low accompanied with a large population of the excited state. Population losses can be suppressed if far-detuned chirped adiabatic two-photon Raman passage methods are employed. Schemes that use chirped laser pulses (CARP), or self-induced adiabatic passage (SCRAP or SIARP) by Stark shifting the transition frequencies, turned out to be very efficient. When it comes to comparing CARP and SCRAP, the former method has the advantage of easy optimization since it has no dependence with respect to pulse shape. Furthermore, for both methods, and unlike STIRAP, the resolved sideband condition imposes less severe constraints on the useful parameter space.

The requirements for all three methods were derived with simulations for a Λ system. Using the results from this simple model, we were able to demonstrate the applicability of CARP in systems with more than two rotational states. For far-detuned transitions, a high-fidelity population mapping from the internal to the motional degrees of freedom is possible. Losses were very low, and our simulations indicate that the fidelity can be further improved by detuning the laser pulses farther from the transition.

In the scheme we propose here, each rotational level is coupled to the excited state by a laser. Due to the large rotational level splitting of light molecules, this means in turn that multiple lasers are required. The number of levels N which have a population larger than the cutoff population P, and therefore the number of required lasers, can be estimated as $N \approx \sqrt{-\ln(2P)k_B T/B}$ for small P. Even though the number of levels N for molecules at room temperature can be of the order of 25, for temperatures of a few Kelvin this reduces to well below ten states. In many experiments, molecular ions can be prepared in low-lying rotational states by employing photoassociation or state selective photoionization in conjunction with supersonic beam expansion or buffer-gas cooling. However, due to the interaction with black-body radiation and collisions, the internal temperature quickly thermalizes. By applying the scheme proposed here, this thermalization can be suppressed to maintain the ground-state population. Additionally, the state mapping can be employed to detect the internal states of the molecule in a nondestructive manner, which is beneficial to high-resolution spectroscopy of molecules.

In conclusion, we have developed a fast scheme for cooling the internal states of single molecules by employing adiabatic passage methods which provide a high efficiency in conjunction with robustness against variations in the parameters of the involved laser pulses.

ACKNOWLEDGMENTS

We thank W. Lange for many helpful comments. This work was supported in part by the European Commission's ITN project FASTQUAST.

[1] J. Ye, H. J. Kimble, and H. Katori, Science **320**, 1734 (2008).

[2] D. I. Schuster, L. S. Bishop, I. L. Chuang, D. DeMille, and R. J. Schoelkopf, e-print arXiv:0903.3552.

[3] D. DeMille, Phys. Rev. Lett. **88**, 067901 (2002).

[4] S. Schiller and V. Korobov, Phys. Rev. A **71**, 032505 (2005).

[5] C. Chin, V. V. Flambaum, and M. G. Kozlov, New J. Phys. **11**, 055048 (2009).

[6] J. J. Hudson, B. E. Sauer, M. R. Tarbutt, and E. A. Hinds, Phys. Rev. Lett. **89**, 023003 (2002).

[7] M. Quack, J. Stohner, and M. Willeke, Annu. Rev. Phys. Chem. **59**, 741 (2008).

[8] J. Doyle, B. Friedrich, R. V. Krems, and F. Masnou-Seeuws, Eur. Phys. J. D **31**, 149 (2004).

[9] H. L. Bethlem and G. Meijer, Int. Rev. Phys. Chem. **22**, 73 (2003).

[10] R. Fulton, A. I. Bishop, M. N. Shneider, and P. F. Barker, J. Phys. B **39**, S1097 (2006).

[11] P. D. Lett, K. Helmerson, W. D. Phillips, L. P. Ratliff, S. L. Rolston, and M. E. Wagshul, Phys. Rev. Lett. **71**, 2200 (1993).

[12] M. Viteau, A. Chotia, M. Allegrini, N. Bouloufa, O. Dulieu, D. Comparat, and P. Pillet, Science **321**, 232 (2008).

[13] J. M. Hutson and P. Soldán, Int. Rev. Phys. Chem. **25**, 497 (2006).

[14] S. A. Rangwala, T. Junglen, T. Rieger, P. W. H. Pinkse, and G. Rempe, Phys. Rev. A **67**, 043406 (2003).

[15] M. S. Elioff, J. J. Valentini, and D. W. Chandler, Science **302**, 1940 (2003).

[16] S. G. Schirmer, Phys. Rev. A **63**, 013407 (2000).

[17] V. Vuletić, J. K. Thompson, A. T. Black, and J. Simon, Phys. Rev. A **75**, 051405(R) (2007).

[18] A. Bartana, R. Kosloff and D. J. Tannor, J. Chem. Phys. **99**, 196 (1993).

[19] A. Bartana, R. Kosloff, and D. J. Tannor, J. Chem. Phys. **106**, 1435 (1997).

[20] A. Bartana, R. Kosloff, and D. J. Tannor, Chem. Phys. **267**, 195 (2001).

[21] G. Morigi, P. W. H. Pinkse, M. Kowalewski, and R. de Vivie-Riedle, Phys. Rev. Lett. **99**, 073001 (2007).

[22] K. Mølhave and M. Drewsen, Phys. Rev. A **62**, 011401(R) (2000).

[23] P. F. Staanum, K. Højbjerre, R. Wester, and M. Drewsen, Phys. Rev. Lett. **100**, 243003 (2008).

[24] J. C. J. Koelemeij, B. Roth, A. Wicht, I. Ernsting, and S. Schiller, Phys. Rev. Lett. **98**, 173002 (2007).

[25] I. S. Vogelius, L. B. Madsen, and M. Drewsen, J. Phys. B **39**, S1267 (2006).

[26] I. S. Vogelius, L. B. Madsen, and M. Drewsen, Phys. Rev. A **70**, 053412 (2004).

[27] J. S. Melinger, S. R. Gandhi, A. Hariharan, D. Goswami, and W. S. Warren, J. Chem. Phys. **101**, 6439 (1994).

[28] S. Chelkowski and G. N. Gibson, Phys. Rev. A **52**, R3417 (1995).

[29] S. Chelkowski and A. D. Bandrauk, J. Raman Spectrosc. **28**, 459 (1997).

[30] V. S. Malinovsky and J. L. Krause, Eur. Phys. J. D **14**, 147 (2001).

[31] D. Grischkowsky and M. M. T. Loy, Phys. Rev. A **12**, 1117 (1975).

[32] L. P. Yatsenko, B. W. Shore, T. Halfmann, K. Bergmann, and A. Vardi, Phys. Rev. A **60**, R4237 (1999).

[33] T. Rickes, L. P. Yatsenko, S. Steuerwald, T. Halfmann, B. W. Shore, N. V. Vitanov, and K. Bergmann, J. Chem. Phys. **113**, 534 (2000).

[34] See N. V. Vitanov, M. Fleischhauer, B. W. Shore, and K. Bergmann, in *Advances in Atomic, Molecular, and Optical Physics*, edited by H. Walther and B. Bederson (Academic, New York, 2001), Vol. 46, p. 55, and references therein.

[35] S. A. Rice and M. Zhao, *Optical Control of Molecular Dynamics* (Wiley, New York, 2000).

[36] G. W. Coulston and K. Bergmann, J. Chem. Phys. **96**, 3467 (1992).

[37] *Atomic and Molecular Beam Methods*, edited by G. Scoles (Oxford University, New York, 1988), Vol. 1.

[38] M. D. Barrett *et al.*, Phys. Rev. A **68**, 042302 (2003).

[39] B. W. Shore, *The Theory of Coherent Atomic Excitation* (Wiley, New York, 1990), Vol. 2.

[40] See, for example, Ref. [41] and the work by J. I. Cirac, R. Blatt, P. Zoller, and W. D. Phillips [Phys. Rev. A **46**, 2668 (1992)], where details for a single transition in the Lamb-Dicke limit are given.

[41] D. Leibfried, R. Blatt, C. Monroe, and D. Wineland, Rev. Mod. Phys. **75**, 281 (2003).

[42] K. Bergmann and B. W. Shore, in *Molecular Dynamics and Spectroscopy by Stimulated Emission Pumping*, edited by H. L. Dai and R. W. Field (World Scientific, Singapore, 1995), Chap. 9, p. 315.

[43] K. Bergmann, H. Theuer, and B. W. Shore, Rev. Mod. Phys. **70**, 1003 (1998).

[44] P. Král, I. Thanopulos, and M. Shapiro, Rev. Mod. Phys. **79**, 53 (2007).

[45] N. V. Vitanov and S. Stenholm, Opt. Comm. **135**, 394 (1997).

[46] N. V. Vitanov and S. Stenholm, Phys. Rev. A **56**, 1463 (1997).

[47] V. I. Romanenko and L. P. Yatsenko, Opt. Comm. **140**, 231 (1997).

[48] In the context of ion traps, see, e.g., D. J. Wineland, J. J. Bollinger, W. M. Itano, and D. J. Heinzen, Phys. Rev. A **50**, 67 (1994), see Sec. VIII.; J. Steinbach, J. Twamley, and P. L. Knight, *ibid.* **56**, 4815 (1997); D. J. Wineland, C. Monroe, W. M. Itano, D. Leibfried, W. E. King, and D. M. Meekhof, J. Res. Natl. Inst. Stand. Technol. **103**, 259 (1998).

[49] As explained by B. W. Shore, K. Bergmann, A. Kuhn, S. Schiemann, J. Oreg, and J. H. Eberly [Phys. Rev. A **45**, 5297 (1992)], the far off-resonant STIRAP process can be seen as a limit of SCRAP or SIARP in the absence of decay. In the presence of decay, the STIRAP process is affected more, due to the involvement of the excited state in the dynamics taking place over a long time.

[50] L. D. Landau, Phys. Z. Sowjetunion **2**, 46 (1932).

[51] C. Zener, Proc. R. Soc. London A **137**, 696 (1932).

[52] Due to the generally different rotational constants, any population in vibrationally excited states is basically unaltered by the mapping process we have presented here. Thus only the vibrational ground state of the molecule is transferred into its rotational ground state.